Assessment of highway pavement concrete suffering from alkali-silica reaction: case study

D. Jóźwiak-Niedźwiedzka✉, A. Antolik

Institute of Fundamental Technological Research, Polish Academy of Sciences, (Warsaw, Poland)
✉:djozwiak@ippt.pan.pl

ABSTRACT: After 15 years of exploitation, numerous instances of damage to the concrete pavement motorway located in northern Germany were observed. Detailed macro and microscopic analysis and determination of mechanical properties were performed on the collected cores. It was found that cracks in the coarse and fine aggregate resulted from advanced alkali-silica reaction. No impact of de-icing agents on the destruction of the concrete pavement was found, while attention was paid to the potential intensification of concrete degradation resulting from the increase in traffic on motorways. The results obtained are a detailed supplement to the German research, as this region (Rostock) has not been analysed before.

KEY WORDS: Alkali-silica reaction; Concrete; Aggregate; Petrographic analysis; Microstructure.

RESUMEN: *Evaluación del hormigón del pavimento de carreteras que sufre de reacción álcali-sílice: caso de estudio.* Se han observado grandes daños después de 15 años de funcionamiento en una carretera pavimentada de hormigón en el norte de Alemania. Se llevaron a cabo análisis macro y microscópicos detallados, así como la determinación de propiedades físicas en los testigos extraídos. Se encontró que fracturas de árido grueso y fino son el resultado de una reacción álcali-sílice avanzada. No se encontró ningún efecto de los agentes descongelantes sobre la destrucción de los pavimentos de hormigón, aunque llamó la atención la posibilidad de intensificación de la degradación del hormigón como resultado del aumento del tráfico en las autopistas. Los resultados obtenidos son un complemento detallado dentro de la investigación alemana, ya que esta región (Rostock) no ha sido analizada antes.

PALABRAS CLAVE: Reacción álcali-sílice; Hormigón; Árido; Análisis petrográfico; Microestructura.

1. INTRODUCTION

Since 1940, when Stanton first reported about the alkali-silica reaction (ASR) (1), this phenomenon associated with severe concrete deformation has been a major durability problem in concrete structures. ASR has been identified worldwide (2, 3), and its occurrence has been considered in detail, including in various types of concrete structures like highway pavements, airfield pavements or dams, but also in bridges, viaducts and buildings (4-7).

Most often, ASR is observed in expressway and highway concrete pavements, where it may result from additional operational factors: dynamic loads from passing trucks and continuous access of alkalis from de-icing agents. It has been found that the loads generated by heavy duty vehicles caused greater concrete damage compared to damage caused by passenger cars. A truck with an axle load of 11.5 tonnes places 280,000 times more strain on traffic routes than a car with an axle load of 0.5 tonnes (8). Evidence of the increase of ASR damage processes due to mechanical pre-damage of the concrete microstructure (increased penetration of de-icing salt and moisture in cyclic pre-damaged concrete) was confirmed (9). Also, the influence of de-icing agents used on concrete pavements, mainly based on chlorides (10), but also formates (11) or acetates (12), contributes to the faster destruction of concrete.

The above test results are confirmed in real environmental conditions. The damage to three concrete pavements of different age (3, 15 and 18 years old) was investigated in Argentina (13), where the main reason for the deterioration of all three was ASR. Hong et al. (14) investigated the cause of highway pavement concrete destruction in South Korea and confirmed that the concrete degradation, which was only four to seven years after construction, occurred as a result of ASR. Frýbort et al. (4) found that serious deterioration of Czech highway concrete pavement was also caused by ASR. The authors concluded that nearly any aggregate used in this region of Europe can be considered as potentially reactive, which was confirmed by the observations of Glinicki et al. (15) and Seyfarth et al. (16), who presented the results of five years of research on German concrete pavements from many different locations.

In recent years, there has been a significant increase in road transport, which is considered the main mode of transport in Germany, and a further increase of about 38% by 2030 is expected (8). Therefore, a problem concerning the durability of German federal highways has arisen. A concrete pavement, which is characterised by a long service life - usually assumed as 30 years - will not be able to meet this requirement. Obvious signs of damage, usually beginning with discoloration in the transverse and longitudinal joints, occurred after 7 to 15 years (8).

The aim of the study presented in this paper was to identify the reaction products developed in the damaged concrete pavement and to determine their causes using mechanical and microscopic tests. The development of the alkali-silica reaction was suspected to be the principal cause of concrete deterioration. In all cases, NaCl was used as a de-icer.

2. MATERIALS

The expressway was built more than 15 years ago and there is no original data on the composition of the concrete. It can only be assumed that the local resources of fine and coarse aggregate were used, as the current German ASR guidelines have been in force for only 9 years (17). The research was carried out on cores cut from the concrete expressway in the vicinity of Rostock. After 15 years of use, the concrete pavement was characterised by significant cracks (Figure 1). From representative locations on damaged sections of the concrete slabs, cores were extracted and were subjected to detailed laboratory tests and analysis.

The drill cores were taken via cracks or joints. The drillings were led from above through the structural concrete of the slabs (in the following also referred to as concrete, which had a thickness of about 265 mm).

FIGURE 1. Surface cracking of concrete highway pavement suspected to be due to ASR.

3. TESTING METHODS

3.1. Visual inspections and macroscopic analysis

The drilled cores were subjected to a thorough visual inspection, photographed (Figure 2) and measured. Macroscopic analysis was performed on halves of 6 cores cut vertically. The remaining core halves were left as control and reference. The homogeneity of the concrete, general composition, type of fine and coarse aggregate as well as entrapped air and cracks were taken into consideration. After macroscopic analysis, the specimens were cut into 30±2 mm sections, polished on SiC powders (180, 320, 600, 1000) and dried at 50°C for 24 h. The Damage Rating Index (DRI) method was used to quantify the internal deterioration of the concrete pavement (18). A petrographic examination was performed using a stereomicroscope at 30x mag. in order to identify and count defects associated with ASR. The assessment was made on the basis of summing up individual factors with different weights adopted in accordance with (18). The higher the DRI value, the higher the ASR-induced concrete degradation rate. The analysis was performed on 6 specimens (10x10 cm).

(a)
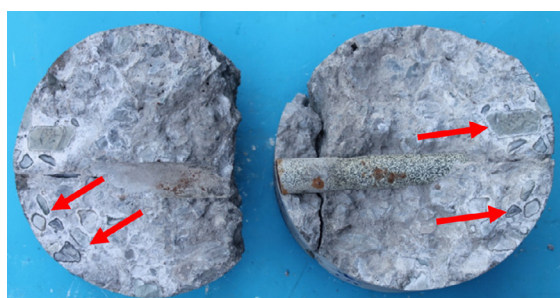
(b)

FIGURE 2. Photograph of the cores: a) jacket surface of core 2 during advanced drying, after immersion in water to make the cracks in the concrete more visible, b) typical signs of ASR - the edges or the fracture surfaces of the aggregates (s. arrows).

3.2. Mechanical properties

In order to determine the compressive strength and the bulk density of the highway pavement concrete, sections of small cores (Ø ≈ 100 mm and 200 mm long) were cut out of each drill core. As in the case of the E-modulus tests, part of these sections were exposed to moist and warm storage (40°C and 100% RH). After cutting and grinding and prior to testing, these specimens were stored under laboratory conditions (23°C and 50% RH until thermo-hygro equilibrium), weighed and measured to determine the bulk density.

To determine the modulus of elasticity, sections 170–200 mm long were cut out of the small cores. Then the end faces of the sections were ground plane-parallel. Afterwards the E-modulus tests were carried out.

The specimens were initially loaded up to the σ_o upper stress of almost 30 MPa. This corresponds to about one third of the average compressive strength of the specimens of 85.4 MPa. Afterwards, the specimens were unloaded to σ_u of about 0.5 MPa. Then two more loading and unloading cycles were applied. Finally, the Young's modulus was determined as the secant modulus from the third rising branch of the respective stress–strain lines.

The E-modulus tests were carried out on specimens stored in laboratory conditions (23°C and 50% RH) and specimens that were exposed beforehand to a moist-warm storage (40°C and 100% RH) to initiate ASR.

3.3. Microscopic analysis

For petrographic analysis, a polarising microscope (Olympus BX51) equipped with a camera and an automatic moving table (Prior ES11BX/B) were used. Thin sections of about 20±2 μm were used for plane-light (PPL) and cross-polarised light (XPL) observations at magnifications from 40 to 400x. The specimens cut from the concrete cores were lapped and then polished (45x30 mm) to identify the alkali-silica gel. A layer of carbon was sprayed onto the samples and a strip of conductive tape was attached to provide conductivity. A scanning electron microscope (SEM) equipped with energy dispersion X-ray analysis (EDX) was used to study the microstructure of the concrete. A Zeiss sigma VP microscope in backscatter mode at an accelerating voltage of 20 kV was used.

4. RESULTS AND DISCUSSION

4.1. Visual inspections and macroscopic analysis

The thickness of the structural concrete of the roadway slabs was from 285 to 247 mm. The drill cores from the structural concrete did not differ from each other with regard to the concrete composition and structural design. The maximum grain size was approx. 32 mm. The aggregate consisted mainly of

crushed, fine-crystalline, siliceous aggregates and sand, as is typical for northern Germany. The concrete contained neither siliceous chalk nor opaline sandstone. The concrete was well compacted. It contained relatively few coarse pores and air-voids due to the air-entraining process. However, in all the investigated core specimens cracks typical of ASR were found (Figure 2). Some of the cracks run through the aggregates, others along the contact zones. As a rule, these cracks run vertically from the upper face of the component to a depth of 50~100 mm and then incline into the direction parallel to the surface. On the fracture surfaces some fractures are visible, running through the coarse aggregates. The edges of the aggregates or the fracture surfaces running through them show reaction edges typical of ASR. The fine parts of the matrix have been torn out by the rolling over of tyres, which was probably caused by high traffic volumes, while the somewhat deeper embedded, coarser grains of sand have remained fixed in the matrix. There were no signs of structural loosening or sanding due to freeze–thaw cycles on any of the surfaces. It is known from the literature (8, 19) that, in the case of permanent access of alkali from de-icing agents and the presence of heavy traffic, which is of particular importance for the stresses of the road structure, the alkali-silica reaction may occur faster. When there is a simultaneous interaction of cyclic freezing and thawing, the concrete deterioration may be more severe. Bérubé et al. (19) revealed that, regardless of the air content, freezing and thawing greatly increased the concrete expansion in the presence of ASR, even after the ASR was almost complete; freezing and thawing also greatly promoted surface cracking.

Summarised results of the calculation of the DRI are presented in Figure 3. The average value of the DRI from six specimens was 384±32, which suggests that the concrete pavement was damaged due to ASR. Sanchez et al. (20) and Fournier et al. (21) suggested a classification of ASR damage exposed to a moist-warm storage for the DRI using the weighting factors proposed by Villeneuve et al. (18), according to which the tested pavement concrete was moderately damaged as a result of ASR (3 on a five-point scale).

4.2. Mechanical properties

The compressive strength for cores cured in moist conditions (40°C, 100% RH) was 87.9±8.1 MPa, and for cores cured in laboratory conditions (23°C, 50% RH) – 82.9±11.2 MPa. The average value was 85.4 MPa. Since the strength of the differently pre-treated test specimens differed only slightly, in the
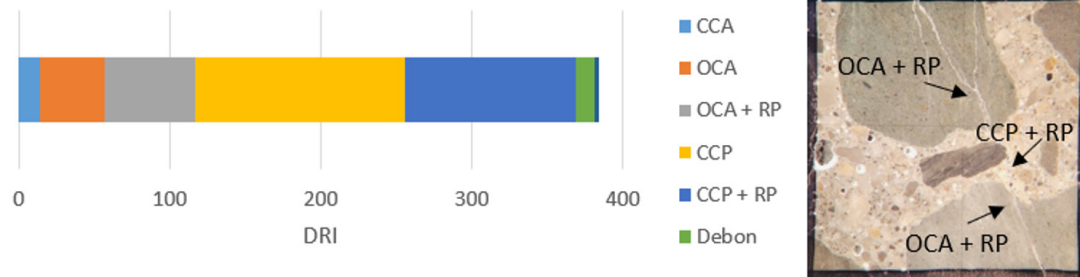
CCA-closed cracks in the coarse aggr. OCA- open cracks or network of cracks in the coarse aggr. OCA+RP-cracks or network of cracks with reaction product in the coarse aggr. CCP-cracks in cement paste. CCP+RP-cracks with reaction product in cement paste. Debon-coarse aggr. deboned
FIGURE 3. Results of petrographic examination for Damage Rating Index calculations performed on the concrete cores and exemplary analysed area 1x1 cm².

TABLE 1. Results of the E module test.

Core no.	1	2	3	4	5	6	7	8
E-Modulus (GPa)	17.3	28.8	24.0	17.1	25.3	24.7	19.8	27.6
Curing conditions	lab. conditions (23°C, 50% RH)				moist warm (40°C, 100% RH)			
Crack damage due to ASR	**	*	***	***	*	**	*	**

* a few, ** strong, *** severe.

following evaluation they were therefore considered as belonging to one and the same population. Taking into account the slimness and diameter of the specimens, these correspond to the compressive strengths of cubes with an edge length of 150 mm.

The determined gross densities were between 2.34 and 2.49 kg/dm³, with an average value of 2.39 kg/dm³. The modulus of elasticity was determined as the increase in the secant modulus from the third stress (including the pre-loading cycle) between the σ_u (upper) and σ_o (lower) stress levels used in the testing cycle, as summarised in the following Table 1.

The modulus of elasticity ranges from 17.1–28.8 GPa, with an average value of 23.1 GPa. The modulus of elasticity itself correlates significantly with the extent of the crack formation, which was described in Table 1 as a few, strong and severe damage due to ASR. Only the modulus of 28.8 and 27.6 GPa determined with two specimens: no. 2 and 8, come close to the values to be expected for a concrete with the strength of approx. 85.6 MPa presented here. For the other values, the modulus lies between 17.1 and 25.3 GPa. Considering the existing compressive strength, these values appear to be clearly too low. Probably the size and cracks network did not significantly affect the strength results, but the changes which suggest internal damage are visible in the values of the modulus of elasticity.

The average compressive strength (85.4 MPa) and the determined gross densities were 2.39 kg/dm³, which was within the range to be expected for concrete of the present quality (22). The calculated parameters according to DIN EN 13791 allow one to classify the investigated structural concrete into the compressive strength class C60/75 according to EN 206-1. Accordingly, it was a high-strength concrete. The average value of the modulus of elasticity was 23.1 GPa, which was below the value according to DIN 1045 (= 40 GPa) (20). The above results are in line with (8, 23), where the substantial reduction in mechanical properties, particularly the tensile strength and the static modulus of elasticity, as a result of ASR was shown. However, no significant compressive strength reductions due to damage caused by the ASR occurred during the moist warm storage. Instead, the concrete achieved a slightly higher strength during the moist warm storage. These increases in strength are generally attributable to the post-hydration process that takes place at these temperatures or to the bonding of crack surfaces with freshly formed ASR gel (24).

4.3. Microscopic analysis

In the concrete cores during petrographic analysis, three main genetic rock types were found: sedimentary, metamorphic rock and mineral clasts (Figure 4). Four aggregate size fractions can be distinguished: 16–32 mm: sandstone and silt, 4–16 mm: sandstone, weakly metamorphosed silt shale (phyllite), limestone, quartz, amphibolite, 0.063–4 mm: quartz, feldspar, limestone, chert, and below 0.063 mm: limestone, quartz, feldspar, amphibolite.

As coarse aggregate, sandstone (Figure 4a), a massive silt with aleuritic microstructure (Figure 4b) and weakly metamorphosed silt shale were found. The sandstone was characterised by well sorted grains with low sphericity, and subrounded. Plagioclase was present as well as carbonate crystals. As a binder, remains of primary clay matrix, secondary siliceous cement and carbonate cement were identified. In the silt, a primary clay matrix was abundant and the secondary matrix was cement. The silt shale was composed of quartz, carbonate, plagioclase, feldspar, muscovite and opaque mineral. As fine aggregate, grains of quartz and limestone were found as well as chert particles (Figure 4c). In most cases, the chert was formed by chalcedony and quartz, but it also contained carbonate.

The pavement concrete was air-entrained to ensure frost resistance. The air-void system was visible on the thin sections, but almost all the air-voids were partially or fully filled by ettringite (Figure 5). However, this should not significantly affect the concrete degradation caused by ASR.

In all the analysed specimens the characteristic ASR map of microcracking was visible, both on whole cores and on micro scale specimens. The microcracks were observed in the fine and coarse ag-
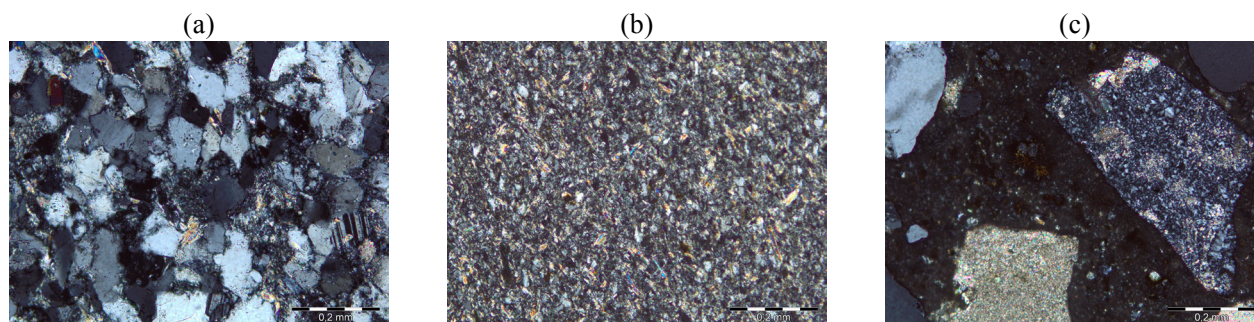

| (a) | (b) | (c) |

FIGURE 4. Cross-sections of coarse aggregate on thin section in XPL: a) sandstone, b) silt and c) fine aggregate: quartz, limestone and chert; scale bar = 0.2 mm.
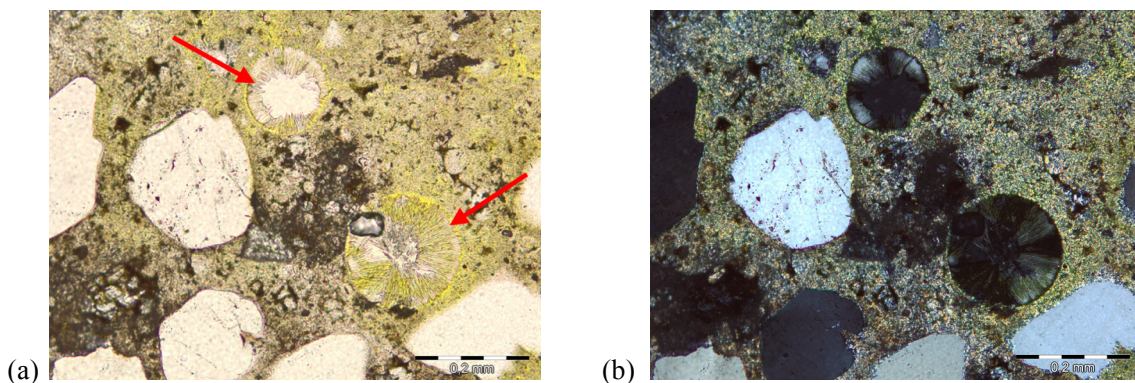
FIGURE 5. Cross-sections of the concrete microstructure: air-voids partially filled with ettringite needles, fine aggregate particles: quartz; a) PPL, b) XPL; scale bar = 0.2 mm.
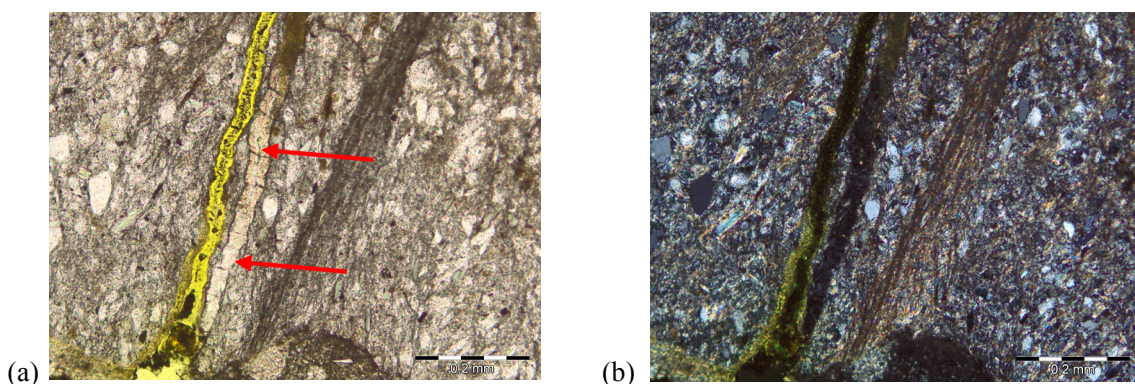

FIGURE 6. Cross-sections of the coarse aggregates: weakly metamorphosed silt shale (phyllite) on thin section with visible ASR gel (red arrows): a) PPL, b) XPL; scale bar = 0.2 mm.

gregate and cement matrix (Figures 6–8). Most of the cracks were propagating from aggregate grains through the cement matrix (Figure 6). They were empty or lined with ASR gel. The cracks located in the coarse and fine aggregate contained Si-Ca-K-Na gel (Figures 6 and 7). The microscopic analysis did not reveal any de-icer ions in the CSH. There was no presence of either chloride ions, ASR gel or Friedel's salt in the cement matrix.

Much lower content of sodium ions compared to potassium ions was found in the alkali-silica gel (Figures 7-8), which may result mainly from the composition of the cement used and from the possible leaching of alkali from the aggregate. The cracks in the aggregate, regardless of its fraction, were of similar size – 30~40 μm, and were mostly filled with ASR gel which flowed into the cement matrix. The ASR gel was in an amorphous (Figure 7) and crystalline (Figure 9) form.

In the analysed concrete cores almost whole reacted grains of fine aggregate were also found (Figure 10). The quartz fine aggregate (probably chert) was converted into Si-Ca-K-Na gel. EDS analysis showed the presence of residues of pure quartz. Additionally, the area seen in Figure 10 was analysed using EDS mapping. There were clearly visible whole grains consist-

ing of ASR gel (stronger indications of K and Na) and point indications from pure quartz (Si). The analysis of the sulfur (S) distribution showed the presence of ettringite in the air-voids and cement matrix.

The presence of ASR products in the cracks in the coarse and fine aggregate grains clearly indicates the relationship of these cracks and the cement matrix with the expansive alkali-silica reaction. It is assumed that the concrete pavement degradation was directly due to the presence of chert (above all chalcedony), siltstone (the potentially reactive element was the siliceous cement) and silt shale. The siliceous cement of siltstones has usually not been connected to a risk of ASR, but a microcrystalline fine-grained quartz in siltstones is potentially ASR susceptible and also generally deleterious in the aggregate for concrete, especially when associated with clay minerals (25). The quartz of the cement was very fine-grained and siltstones strongly dominated in the aggregate by volume. Sand grains were mainly monomineral. However, they also contained reactive forms of quartz, which was found using thin section analysis and confirmed by SEM analysis. The sand particles were partially or completely converted into ASR gel, which clearly confirms their ASR potential (26). The ASR ceases when the reactive aggregates, the hydroxyl, or the al-

kalis' sodium and potassium ions are exhausted (27). And although the alkali-silica gel has a much lower Na content compared to K, which may suggest no effect of the NaCl de-icer (or the use of cement with a high K_2O content), the reactive minerals in the aggregate in combination with cement alkali and moisture caused significant damage to the concrete. No presence of Friedel's salt was found, but its formation, which was assumed earlier to increase the sodium concentration in the concrete pore solution, turned out not to be required for ASR and does not result in an increase of the pH (8). Bérubé et al. (28) showed that the high sodium concentration in the near-surface layer of the concrete might not cause severe ASR owing to a decreased OH^- concentration in this area. Heising et al. (29) stated that the chloride binding on hydrated cement phases and the corresponding release of OH^- ions does not significantly promote ASR.
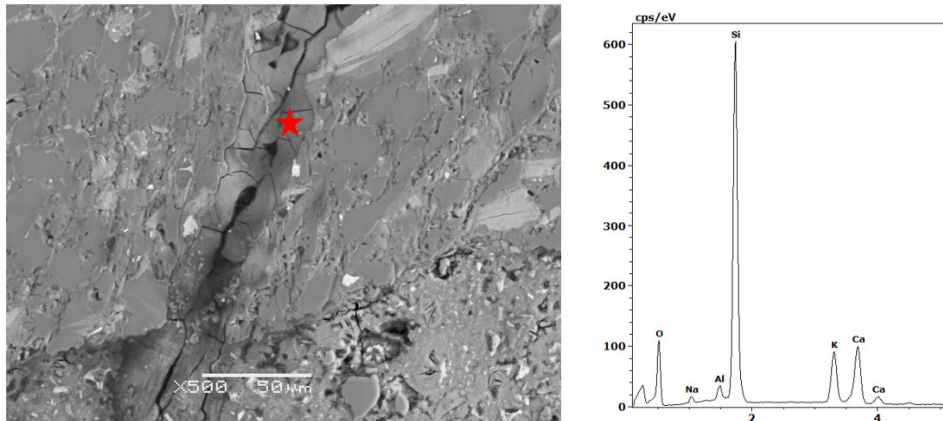

FIGURE 7. Scanning electron micrograph of the cracked coarse aggregate grain (phyllite) filled with Si-Ca-K-Na gel.
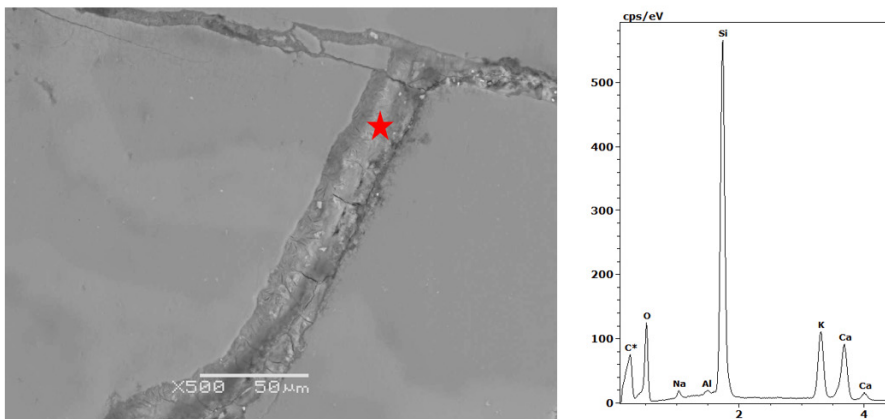

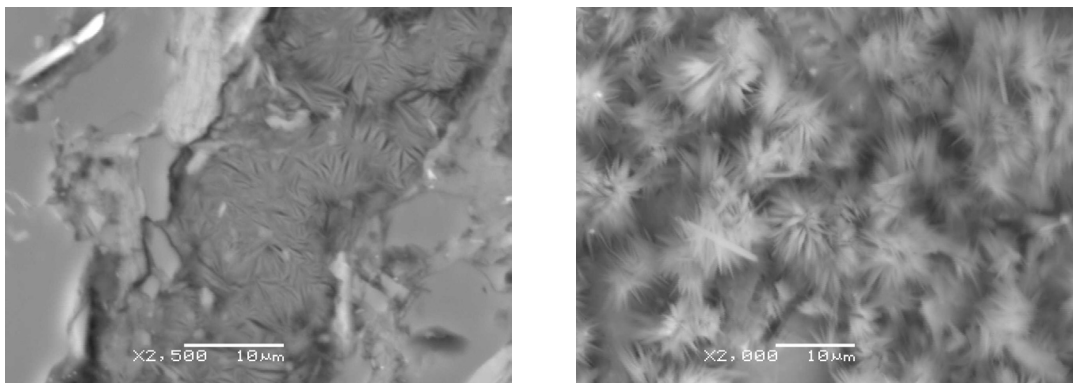FIGURE 8. Scanning electron micrograph of the cracked fine aggregate grain (chert) filled with Si-Ca-K-Na gel.

FIGURE 9. ASR gel on a: a) polished surface and b) fresh fracture surface; SEM, scale bar = 10 μm.
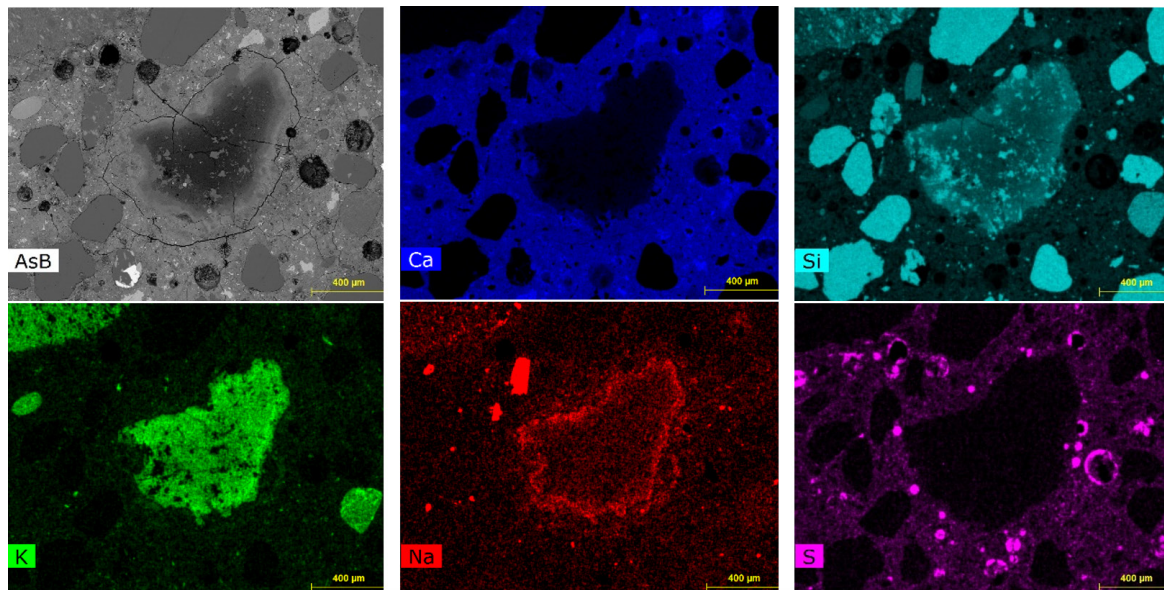
FIGURE 10. EDS mapping of the reacted aggregate grain (partially converted into an ASR gel).

Previous research on degraded pavement concrete (4, 13-15) presented similar observations regarding the ASR as a cause of its destruction; however, they mentioned other reactive aggregates. Rocks such as black shales, green schists and metabasalts used as concrete aggregate revealed the ASR potential (4). Also a strained and microcrystalline quartz as well as volcanic glass were recognised as reactive components (13), as well as black shale and sea-dredged natural sand (14) and a quartzite aggregate (15).

Alkali-silica reaction has been identified in more than 50 countries worldwide (2), but it should be noted that the types of aggregates that caused ASR are very different at these sites. For example, in northern Europe, Danish aggregate is young sedimentary rock and Icelandic aggregate is young volcanic rock, while in Sweden and Norway, old crystalline rock is the main source of aggregate (2).

However, one should also pay attention to the research methods. Seyfarth et al. (16) stated that at highway sections built after 2005, a sufficiently low ASR potential was found. This has been explained by the effectiveness of the new regulations for preventing ASR in highway pavement concrete in Germany. The research results are consistent with the above statement.

The results for cores taken from the damaged concrete pavement, improved test methods and the development of national methods of preventing the alkali-silica reaction in concrete will contribute to the avoidance of reactive aggregate in the construction of durable concrete pavements.

CONCLUSIONS

Highway concrete pavement with various aggregates from northern Germany was investigated with respect to the deterioration caused by alkali-silica reaction.

The following conclusions can be drawn:
- On the basis of petrographic analysis, cracks were identified in coarse aggregate - sandstone and schist, and in fine aggregate grains - quartz sand. A reactive form of quartz (chalcedony) has been identified in the chert particles.
- Amorphous and crystalline gel-like products present in cracks in coarse and fine aggregate consisted of pure potassium-sodium-calcium silicate, which is commonly equated with ASR.
- There was no effect of the NaCl de-icer on the degradation of concrete by inducing or accelerating the ASR, which was visible in the composition of the ASR gel.
- The Damage Rating Index was 384, which clearly confirms the petrographic observations and suggests ASR as the main cause of the destruction of the concrete pavement.
- No significant compressive strength reduction was found; however, a substantial decrease in the modulus of elasticity was shown, which may suggest internal damage in the concrete pavement, not only related to ASR.

AUTHOR CONTRIBUTIONS:

Conceptualization: D. Jozwiak-Niedzwiedzka. Formal analysis: D. Jozwiak-Niedzwiedzka, A. Antolik. Funding acquisition: D. Jozwiak-Niedzwiedzka, A. Antolik. Investigation: D. Jozwiak-Niedzwiedzka, A. Antolik. Methodology: A. Antolik. Resources: D. Jozwiak-Niedzwiedzka. Supervision: D. Jozwiak-Niedzwiedzka. Validation: D. Jozwiak-Niedzwiedzka, A. Antolik. Writing, original draft: D. Jozwiak-Niedzwiedzka. Writing, review & editing: D. Jozwiak-Niedzwiedzka, A. Antolik.

REFERENCES

1. Stanton, T.E. (1940) Expansion of concrete through reaction between cement and aggregate; Proc. of the ASCE 66 (10), 1781–1811.
2. Pyy, H.; Holt, E.; Ferreira, M. (2011) An initial survey on the occurrence of alkali aggregate reaction in Finland, Customer Report VTT-CR-00554-12, pp. 27.
3. Menéndez, E. (2022) Special Issue, 2022 International Conference on Alkali-Aggregate Reaction in Concrete (16th ICAAR), *Mater. Construcc* 72 (346), ed023 https://doi.org/10.3989/mc.2022.v72.i346.
4. Frýbort, A.; Všianský, D.; Štulířová, J.; Stryk, J.; Gregerová, M. (2018) Variations in the composition and relations between alkali-silica gels and calcium silicate hydrates in highway concrete. *Mater. Charact.* 137, 91–108.
5. Muñoz, J.F.; Balachandran, Ch.; Arnold, T.S. (2021) Alkali-silica reactivity of aggregates from airfield pavements and its correlation with historic field performance. *Int. Airfield Highway Pavem. 2021.* https://doi.org/10.1061/9780784483527.012.
6. Comi, C.; Fedele, R.; Perego, U. (2009) A chemo-thermo-damage model for the analysis of concrete dams affected by alkali-silica reaction. *Mech. Mater.* 41 [3], 210–230. https://doi.org/10.1016/j.mechmat.2008.10.010.
7. Lahdensivu, J.; Köliö, A.; Husaini, D. (2018) Alkali-silica reaction in Southern-Finland's bridges. *Case Stud. Constr. Mater.* 8, 469–475. https://doi.org/10.1016/j.cscm.2018.03.006.
8. Mielich, O. (2019) Alkali-silica reaction (ASR) on German motorways: an overview. *Otto-Graf-J.* 18, 197–208.
9. Wiedmann, A.; Weise, F.; Kotan, E.; Müller, H.S.; Meng, B. (2017) Effects of fatigue loading and alkali–silica reaction on the mechanical behavior of pavement concrete. *Struct. Concr.* 18, 539–549. https://doi.org/10.1002/suco.201600179.
10. Jain, J.; Olek, J.; Janusz, A.; Jóźwiak-Niedźwiedzka, D. (2012) Effects of deicing salt solutions on physical properties of pavement concretes. *Transp. Res. Recor.* 2290 [1], 69-75 https://doi.org/10.3141/2290-09.
11. Giebson, C.; Seyfarth, K.; Stark, J. (2010) Influence of acetate and formate-based deicers on ASR in airfield concrete pavements. *Cem. Concr. Res.* 40, 537–545. https://doi.org/10.1016/j.cemconres.2009.09.009.
12. Balachandran, C; Olek, J.; Rangaraju, P.R.; Diamond, S. (2011) Role of potassium acetate deicer in accelerating alkali–silica reaction in concrete pavements: Relationship between laboratory and field studies. *Transp. Res. Recor.* 2240 [1], 70–79. https://doi.org/10.3141/2240-10.
13. Marfil, S.A.; Maiza, P.J. (2001) Deteriorated pavements due to the alkali-silica reaction: A petrographic study of three
14. cases in Argentina. *Cem. Concr. Res.* 31, 1017–1021. https://doi.org/10.1016/S0008-8846(01)00508-7.
14. Hong, S.H.; Han, S.H.; Yun, K.K. (2007) A case study of concrete pavement deterioration by alkali-silica reaction in Korea. *Int. J. Concr. Struct. Mater.* 1 [1], 75–81.
15. Glinicki, M.A.; Jóźwiak-Niedźwiedzka, D.; Antolik, A.; Dziedzic, K.; Dąbrowski, M.; Bogusz, K. (2022) Diagnosis of ASR damage in highway pavement after 15 years of service in wet-freeze climate region. *Case Stud. Constr. Mater.* 17, e01226. https://doi.org/10.1016/j.cscm.2022.e01226.
16. Seyfarth, K.; Giebson, C.; Ludwig, H. (2022) ASR related service life estimation for concrete pavements. *Mater. Construcc.* 72 [346], e287. https://doi.org/10.3989/mc.2022.15921.
17. DAfStb-Richtlinie, Vorbeugende Maßnahmen gegen schädigende Alkalireaktion im Beton, (Alkali-Richtlinie), Oktober 2013, pp. 48.
18. Villeneuve, V.; Fournier, B.; Duschene, J. (2012) Determination of the damage in concrete affected by ASR – The damage rating index (DRI). Proc. 14th ICAAR, Austin, USA.
19. Bérubé, M-A.; Chouinard, D.; Pigeon, M.; Frenette, J.; Boisvert, L.; Rivest, M. (2002) Effectiveness of sealers in counteracting alkali-silica reaction in plain and air-entrained laboratory concretes exposed to wetting and drying, freezing and thawing, and salt water. *Can. J. Civ. Eng.* 29 [2], 289–300. https://doi.org/10.1139/l02-011.
20. Sanchez, L.F.M.; Fournier, B.; Jolin, M.; Mitchell, D.; Bastien, J. (2017) Overall assessment of Alkali-Aggregate Reaction (AAR) in concretes presenting different strengths and incorporating a wide range of reactive aggregate types and natures. *Cem. Concr. Res.* 93, 17–31. https://doi.org/10.1016/j.cemconres.2016.12.001.
21. Fournier, B.; Fecteau, P.L.; Villeneuve, V.; Tremblay, S.; Sanchez, L. (2015) Description of petrographic features of damage in concrete used in the determination of the DRI. Québec: Département de géologie et de génie géologique, Université Laval.
22. Rostàsy, F.S. (1983) Baustoffe. Verlag W. Kohlhammer, Stuttgart – Berlin – Köln – Mainz. pp. 243.
23. Reinhardt, H-W; Mielich, O. (2012) Mechanical properties of concretes with slowly reacting alkali sensitive aggregates. Proc. 14th ICAAR, Austin, USA.
24. Bödeker, W. (2003) Alkalireaktion im Bauwerksbeton – Ein Erfahrungsbericht. Deutscher Ausschuß für Stahlbeton, Heft 539, Beuth Verlag GmbH, Berlin-Wien-Zürich, 1. Auflage.
25. Vola, G.; Berra, M.; Rondena, E. (2011) Petrographic quantitative analysis of ASR susceptible Italian aggregates for concrete. Proc. 13th Euroseminar on Microscopy Applied to Building Materials (EMABM 2011).
26. Jóźwiak-Niedźwiedzka, D.; Antolik, A.; Dziedzic, K.; Gméling, K.; Bogusz, K. (2021) Laboratory investigations on fine aggregates used for concrete pavements due to the risk of ASR. *Road Mater. Pavem. Design.* 22 [12], 2883–2895, https://doi.org/10.1080/14680629.2020.1796767.
27. Fernandes, I.; Noronha, F.; Teles, M. (2004) Microscopic analysis of alkali–aggregate reaction products in a 50-year-old concrete. *Mater. Charact.* 53 [2–4], 295–306, https://doi.org/10.1016/j.matchar.2004.08.005.
28. Bérubé, M.A.; Dorion, J.F.; Duchesne, J.; Fournier, B.; Vézina, D. (2003) Laboratory and field investigations of the influence of sodium chloride on alkali-silica reactivity. *Cem. Concr. Res.* 33, 77–84. https://doi.org/10.1016/S0008-8846(02)00926-2.
29. Heisig, A.; Urbonas, L.; Beddoe, R.E.; Heinz, D. (2016) Ingress of NaCl in concrete with alkali reactive aggregate: effect on silicon solubility. *Mater. Struct.* 49, 4291–4303. https://doi.org/10.1617/s11527-015-0788-y.